Original

Nagaram, A.B.; Ebel, T.:

Development of Ti-22Nb-xZr Using Metal Injection Moulding for Biomedical Applications

Key Engineering Materials, Powder Metallurgy of Titanium II (2016)
Trans Tech Publications

DOI: 10.4028/www.scientific.net/KEM.704.334

Key Engineering Materials
ISSN: 1662-9795, Vol. 704, pp 334-342
doi:10.4028/www.scientific.net/KEM.704.334

Submitted: 2015-10-23
Revised: 2016-02-09
Accepted: 2016-02-25
Online: 2016-08-12

Development of Ti-22Nb-xZr using Metal Injection Moulding for Biomedical Applications

Anok Babu Nagaram[1,2,a *], Thomas Ebel[2,b]

[1]Materials Science, Technical University of Darmstadt, Alarich-Weiss-Straße 2, 64287 Darmstadt, Germany

[2]Materials Design and Characterisation, Helmholtz-Zentrum Geesthacht, Max-Planck-Str. 1, 21502 Geesthacht, Germany

[a]anoknagaram@gmail.com, [b]thomas.ebel@hzg.de

Keywords: Metal Injection Moulding, titanium, beta-alloys, zirconium, carbide reduction, biomedical implant materials

Abstract. Research on biomaterials is connected inherently with the various aspects of materials science, chemistry, biology and medicine. Frequently used biomaterials for implants are titanium alloys because of their high corrosion resistance and biocompatible behaviour together with high strength and low density. One main characteristic property for the consideration of a potential implant material is the Young's modulus which should correspond to that of human bone (4~30 GPa) as close as possible. β-Ti alloys exhibit currently the lowest value of typically 60 to 80GPa. β-Ti phase is stabilized with additive elements such as Mo, Ta, Hf and Nb. In particular, Ti-Nb alloys can exhibit a Young's modulus around 50 to 60 GPa. Metal Injection Moulding (MIM) is a promising production technology because it overcomes the productivity and shape limitations of traditional powder compaction methods. However, formation of carbide precipitates at the grain boundaries deteriorating the ductile behavior of the materialhas become a challenge in MIM. Recent research using MIM on Ti-22Nb with the addition of Zr has revealed the reduction of carbide precipitates. In this study, different amounts of zirconium were added varying between 2 to 10 wt%. Samples produced with 10% Zr revealed the highest tensile strength of 840 MPa. In addition, specimens with higher zirconium content showed the highest ductility. XRD measurements revealed an increase in lattice constant effecting an increase of the carbon solubility of the Ti-matrix and, thus, a reduction of the carbide precipitation.

1 Introduction

Functioning of bone joints such as hip, knee and shoulders is delicate and complicate and deteriorate with increasing age [1-2]. If implants are needed for replacement, artificial biomaterials come into application. It is estimated that 70%-80% of biomedical implant materials are made of metallic materials [3].

Titanium alloys are widely used materials for bone replacement due to their outstanding combination of biocompatible behaviour, high strength to weight ratio, high corrosion resistance and a rather low value of Young's modulus, closer to that of natural bone than that of e.g. stainless steel or cobalt-chromium alloys. This has a positive effect on reduction of the stress shielding effect [4-6].

Commercially pure (CP) titanium and Ti-6Al-4V are today the mostly used materials for synthesis of medical prostheses with good biocompatibility. Nevertheless, there are some limitations for the use of pure titanium and commonly used Ti-alloy (Ti-6Al-4V) for biomedical applications such as the release of neurotoxicity of aluminium (Al) and toxicity of vanadium (V) in the human could cause the risk of long term health problems. Common α-Ti alloys tend to show either cytotoxicity or incompatibility as implant materials known as 'stress shielding effect' and lead to poor osseointegration and loosening of the implant [7-10]. β-phase Ti alloys are most suitable as biomaterial implant material, because, firstly, they exhibit just between 60 and 80 GPa of Young's modulus [11]. On rapid cooling from high temperatures, ß-phase microstructures can be retained in

metastable β-Ti alloys providing a significantly lower Young's modulus than the alpha phase. Secondly, they can be produced using only non-toxic or critical elements. So, β-Ti alloys or near β-Ti alloys have been developed such as Ti-Ta alloys, Ti-Mo alloys and Ti-Hf alloys but Ti-Nb alloys are an unique combination of material that stabilizes the β-phase in Ti alloys and exhibit the lowest Young's modulus of 50 to 60 GPa [12-17].
Processing of Ti and its alloys either by machining or casting is expensive. On the other hand, Metal Injection Moulding (MIM) technique offers possibilities for cost reduction and became more and more attractive during the recent years. In addition to its economic advantage, MIM also offers high design flexibility of the components.
However, formation of titanium carbide precipitates at the grain boundaries due to reaction of Ti-atoms with the polymeric binder leads to brittle behaviour of the metal injection moulding (MIM) material [18].Further research was carried out by Beißig [19] to reduce the amount of carbides using several elemental powders such as boron, tantalum and zirconium as addition. Addition of zirconium has revealed positive results for the reduction of carbide precipitates. In this study the mechanism for the positive effect of zirconium on the carbide precipitation in MIM processed Ti-22Nb alloys was investigated.

2 Experimental Procedures

2.1 Powder Processing and MIM

Different amounts of zirconium powder (<45 μm) produced by TLS Technik, Germany, were mixed with titanium powder (<45 μm) produced by TLS Technik, Germany and niobium powder (0-45 μm) produced in-house by inert gas atomisation. Powder blends of the composition Ti-22Nb-xZr (x=0, 2, 4, 6, 8, 10) were produced by MIM process.Initially, these different compositions of metallic powders were mixed with a binder system (paraffin wax, polyethylene-vinylacetate co-polymer and stearic acid). The resulting feedstock contains 10 wt% of this binder system corresponding to about 35 vol%.

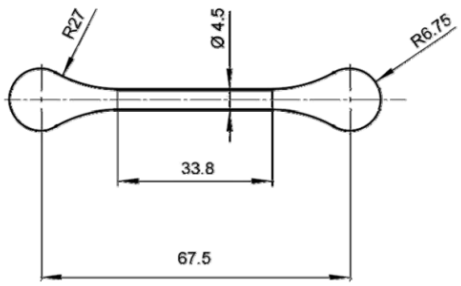

Fig.1 Tensile test specimen according to ISO 2740. Dimensions shown are in millimeters

The feedstock was mixed under heat input of 120 °C in a Z-blade kneader until a homogeneous mixture was reached. After granulation tensile specimens according to ISO 2740 (Fig. 1) were preparedon a conventional injection moulding machine (Arburg Allrounder 320S). These specimens are called green parts.

2.2 Debinding and Sintering

Debinding of the green parts was carried out in two steps. Chemical debinding was applied in hexane at 40°C for 15 h for all produced specimens. This process is carried out to remove atleast one component (paraffin wax, stearic acid) of binder from the specimen. The specimens obtained after chemical debinding are called brown parts.
Thermal debinding and sintering was conducted in a single cycle on XERION XVAC 1600 furnace with tungsten heating elements and shield packs of molybdenum. Thermal debinding was carried out for 4 h in 2 steps at 450°C and at 600°C. Subsequently, the sintering process was performed at a temperature of 1500°C for 4 h under high vacuum ($<10^{-4}$ mbar)followed by controlled furnace

cooling at 10 K/min. Dimensional measurements and weight of specimens were recorded for green parts, brown parts and sintered parts. Fig.2 shows the green specimen and the sintered specimen in comparison.

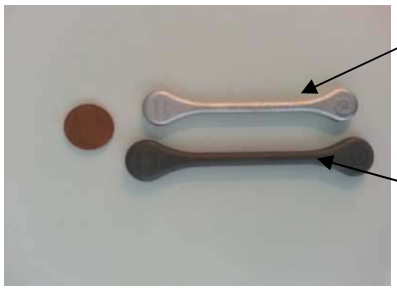

Fig.2 Green specimen and as-sintered specimen

2.3 Materials Characterization

The Archimedes' technique (SartoriousMaster^{pro}, Germany) was used to measure the bulk density of the specimens after sintering. Ethanol was used as immersion medium. Porosity is calculated according to the following equations.

$$\frac{1}{\rho_{theo}} = \frac{x}{\rho_{Ti}} + \frac{y}{\rho_{Nb}} + \frac{z}{\rho_{Zr}} \quad (1)$$

x = mass fraction of Ti; y = mass fraction of Nb; z = mass fraction of Zr; ρ_{theo} = theoretical density of the alloy; ρ_{Ti} = density of titanium; ρ_{Nb} = density of niobium; ρ_{Zr} = density of zirconium

$$\text{Total porosity of the alloy} = 1 - \left(\frac{\rho_{arch}}{\rho_{theo}}\right) \quad (2)$$

ρ_{arch} = Archimedes' density of the alloy

Amount of impurities such asoxygen and carbon in the specimens are measured using O_2 -u - N_2- Analysator LECO-TC and C - u - S- Analysator LECO-CS instrument.

The microstructure of the sintered specimens was examined using optical microscopy (Olympus PMG3) while phases and topography were characterized by scanning electron microscopy (TESCAN-VEGA 3).Carbide area fraction and mean grain sizes were measured using Olympus Soft Image Solution, AnalySISPro on optical micrographs. Grain size measurement was conducted using the method linear intercept technique (ASTM E112-96). For grain size measurements, specimens were etched with Kroll's etching agent (96 ml distilled water, 6 ml HNO_3 and 2 ml HF) for 12 sec for enhancing the visibility of the grain boundaries.

Tensile properties such as tensile strength, elongation and Young's modulus were measured by using a tensile testing machine (SchenckTrebel RM 100 Universalprüfmaschine, Germany) with a Zwick DUPS electronic testing system with maximum load bearing of 100 kN and a strain rate of 1.2 x 10^{-5} s^{-1}. Measurements were carried out on the dog bone tensile specimens in the as-sintered conditions. The average of at least 5 samples from each composition was calculated.

XRD analysis was conducted using SEIFERT XRD 3003 PTS diffractometer at the Deutsches Elektronen Synchrotron (DESY) in Hamburg, Germany, along with corresponding RayfleX (Version:2407) software producing the diffractogram in 2 dimensions such as theta and intensity. Lattice parameters of the samples were measured using Bragg's law equations for BCC and HCP structures.

$$n\lambda = 2d\sin\theta \quad (3)$$

$$\frac{\lambda^2}{4a^2} = \frac{sin^2\,\theta_{hkl}}{h^2+k^2+l^2} \quad (4)$$

$$d = \frac{a}{\sqrt{N}} \quad (5)$$

λ = wave length of the ray, d =spacing between layers of atoms, θ = angle between the incident rays and the surface of the crystal, a = lattice parameter, $N^2 = h^2+k^2+l^2$

3 Results and Discussion

3.1 Effect of zirconium on porosity

The effect of zirconium on porosity in dependence on the different compositions fabricated using MIM method is shown in Fig.3. It can be seen that porosity increases from 3.1% to 3.6% as the zirconium is added to the Ti-22Nb alloy.

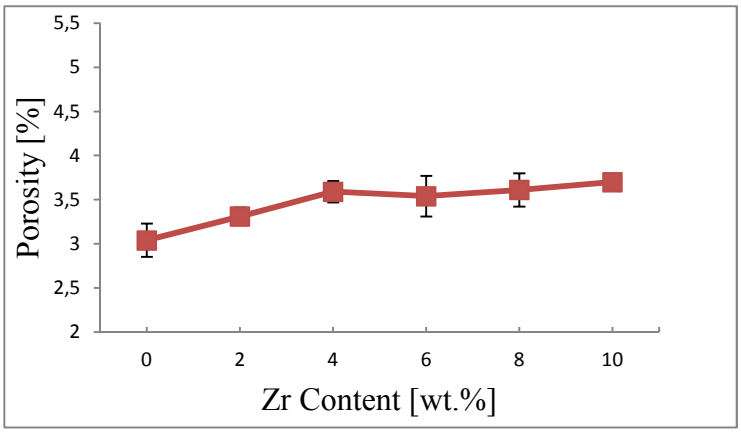

Fig.3 Effect of zirconium on porosity of Ti-22Nb alloy

Even if the change is rather small, it can be noted that the blended elemental approach has a significant effect on the porosity. Mixing three elemental powders require much of diffusion between the particles to get a homogeneous microstructure, thus, hindering the sintering itself. However, all porosity values obtained in this study are rather low when compared to the previous work [19] carried out on Ti-22Nb using MIM method.

3.2 Microstructure

The microstructure of the Ti-22Nb and Ti-22Nb-10Zr alloy prepared by MIM is shown in Fig.4. Optical microstructures displayed the presence of carbides (long band structures, identified in a previous work [18]) and pores. Various sizes and shapes of pores are observed. Pores are uniformly distributed throughout the material. In Fig.4(a) a high amount of carbide precipitates is clearly visible, whereas, with the increase in zirconium content number and size of the carbides decreased as seen in Fig.4(b).

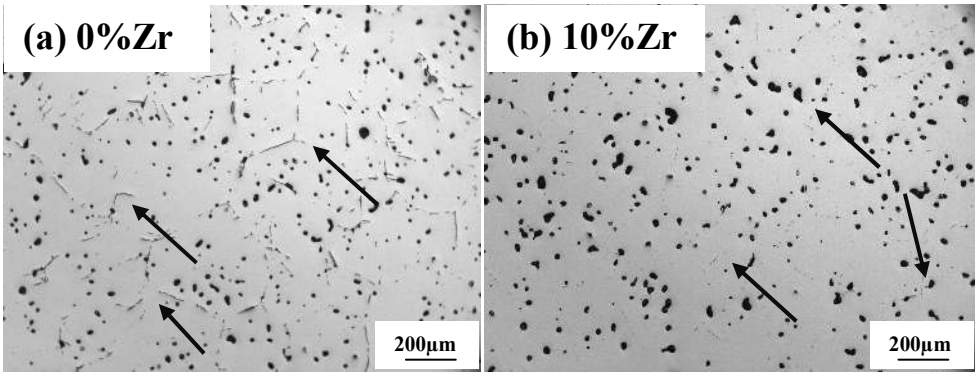

Fig.4 Optical micrographs of (a) Ti-22Nb and (b) Ti-22Nb-10Zr

The mean grain sizes of the sintered specimens of all compositions range from 299±143 µm to 225±111 µm as shown in Fig.5.

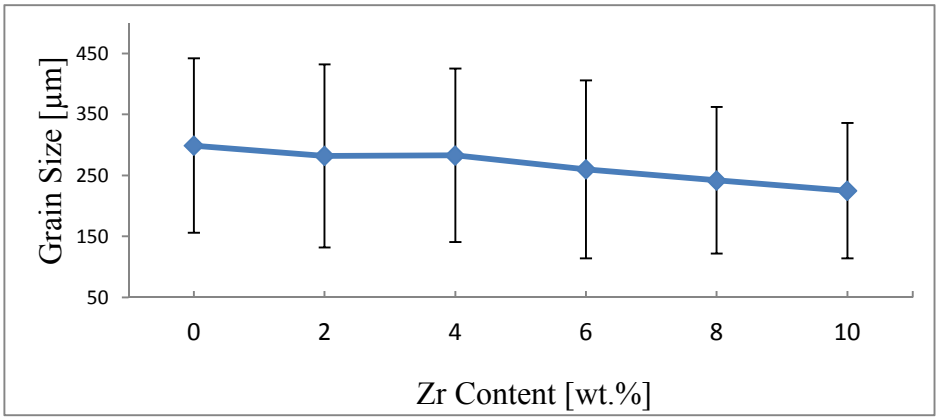

Fig.5 Grain size measurements of Ti-22Nb-(0, 2, 4, 6, 8, 10)Zr alloys

With the increase in zirconium content small effect of grain refinement is observed. The reason for this reduction is not clear, but there may be possibility of newly formed particles that hinders the grain growth.

3.3 Impurity contents and Carbide area fraction

Fig.6(a) shows the contents of carbon and oxygen in the sintered specimens of Ti-22Nb and Ti-22Nb-(2, 4, 6, 8, 10)Zr. The carbon content of all compositions are close to each other and valued around 0.05 wt%, suggesting that the contamination of carbon from the sintering atmosphere was constant. The oxygen contents of the sintered specimens were also close to each other with less than 0.2 wt%.

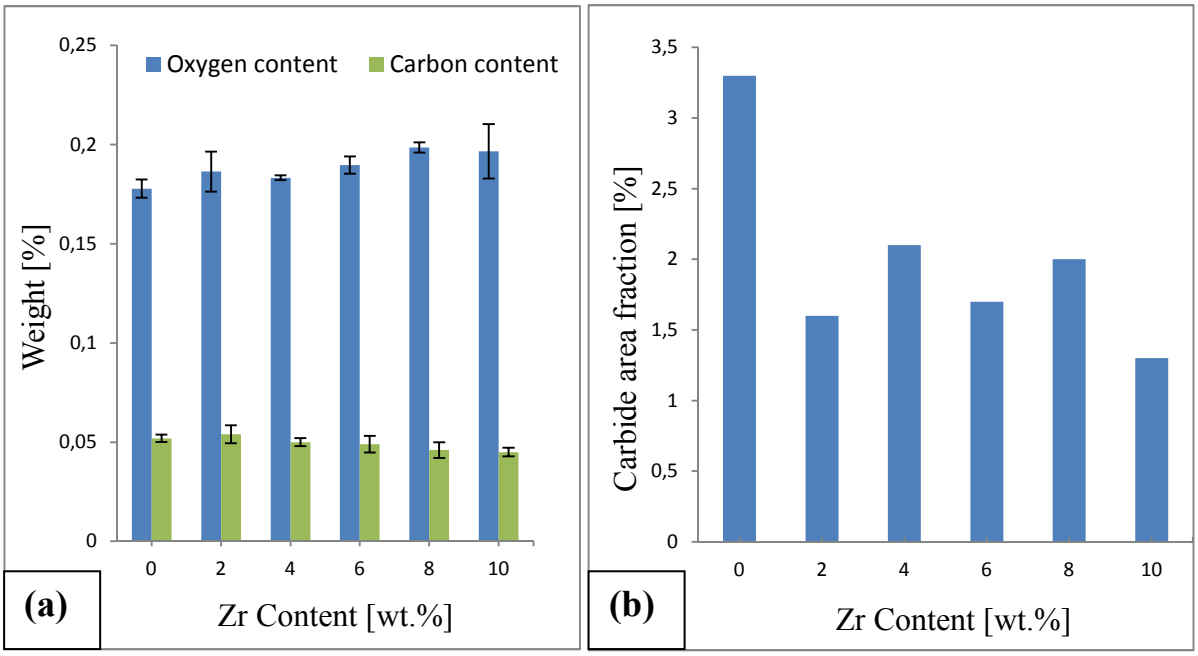

Fig.6(a) Contents of carbon and oxygen and Fig.6(b) Carbide area fraction in sintered specimens of Ti-22Nb-(0,2,4,6,8,10)Zr

The dependence of the measured carbide area fraction on zirconium content is shown in Fig. 6(b). It reveals that carbide precipitates were observed in all compositions, but the highest amount of carbides was determined in the pure base alloy Ti-22Nb. The carbide area fraction decreases from 3.3% to 1.3% by adding 10wt% zirconium. The carbide area fraction is reduced gradually which can be explained by an increase in solubility of carbon inside the matrix when zirconium is added to Ti-22Nb alloy.

3.4 Tensile properties

The tensile properties of Ti-22Nb and Ti-22Nb-(2, 4, 6, 8, 10)Zr are presented in Fig.7. It reveals that yield strength, ultimate tensile strength and elongation increase with increasing amount of zirconium (wt%) in Ti-22Nb, while Young's modulus maintained a rather constant value (~74 GPa) for all the compositions. The ultimate tensile strength gradually increased from 781 MPa to 851 MPa and yield strength increased from 681 MPa to 740 MPa. Elongation to fracture increased from 2.7 % to 4.8 % as zirconium is added to the base alloy. Compared to the previous study [19] a significant improvement in ductility was achieved.

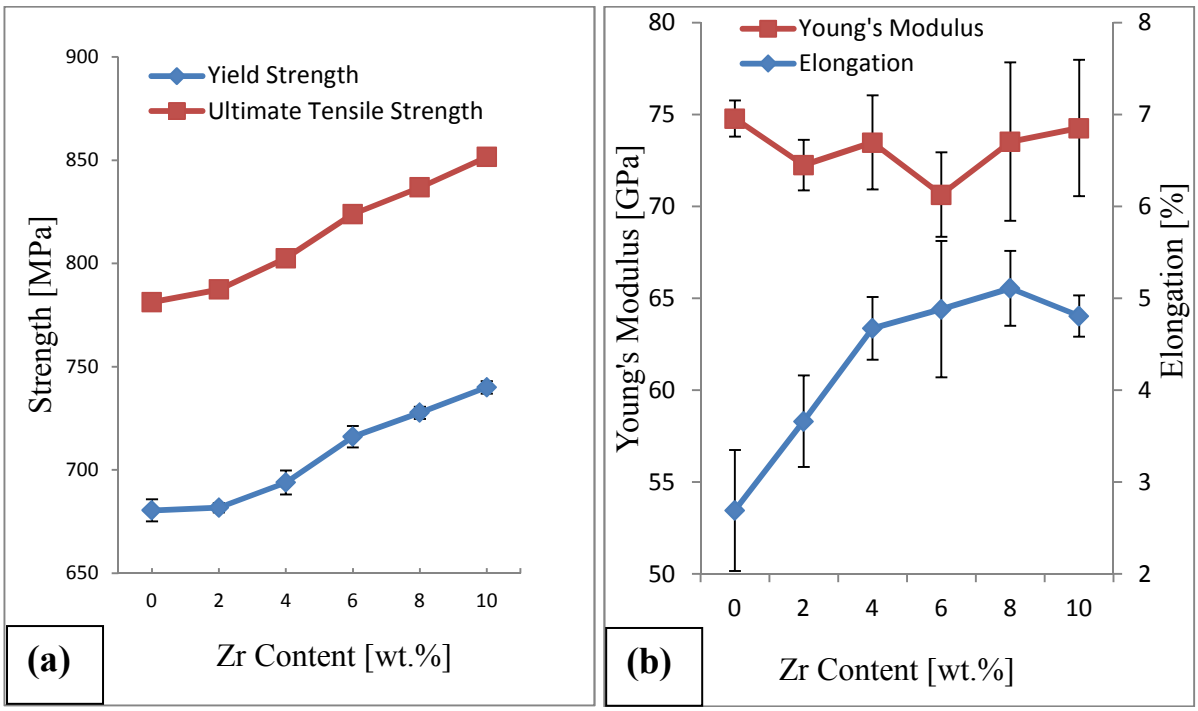

Fig.7 Tensile properties of Ti-22Nb-(0, 2, 4, 6, 8, 10)Zr (a) Tensile strength and (b) Young's modulus and elongation to fracture.

The increase in strength of the samples can be assumed to be mainly due to the effect of solid solution hardening by alloyinghindering the mobility of the dislocation's movement by local distortion of the crystal lattice [20].

Furthermore, the decreasing grain size as seen in Fig.5 may also influence the strength of the alloy. In a study Salishchev et al reported that strengthening of Ti and Ti alloys is observed with the reduction of grain size [21].

As presented in Fig.6(b), the reduction of carbide area fraction could be explained by an increase in carbon solubility of the matrix when zirconium is added to Ti-22Nb alloy. It is reported [22] that solved carbon increases the strength of titanium. Furthermore, it can be assumed that new compounds such as zirconium carbides or titanium zirconium carbides are formed which might act as precipitation hardener. All these factors may also contribute to an increase of strength. However, precipitation hardening by possible smaller carbides in Ti-22Nb-10Zr cannot be discussed in the frame of this study because necessary TEM investigations are missing to prove their existence.

Porosity has a detrimental effect on the strength of the materials due to the influence of the reduced cross section area. So, if porosity can be reduced further increase of strength can be expected.

On the basis of the experiments shown it can be assumed that the increase in ductility is mainly due to the reduction of the amount of carbides as shown in Fig. 6(b). In general, due to their rather low carbon solubility,titanium alloys with carbon content more than about 0.05 to 0.1% tend to the formation of excess carbide precipitation leading to embrittlement [22]. From Fig.6(a), it is noted that the carbon content in all the compositions is the same, so it can be assumed that the decrease of carbides is an effect of increased carbon solubility by Zr addition. Ductility of Ti and Ti alloys can also be enhanced as an effect of reduction in grain size [24] as shown in Fig.5.

Fig.7(b) reveals that neither alloying of Ti-22Nb alloy with addition of Zr in the given range nor the small change in porosity from 3.1% to 3.6% show a clear effect on the Young's modulus.

3.5 XRD analysis

The possible effect of zirconium on the lattice constant is discussed using XRD patterns, shown in Fig.8. It can be seen that only the peaks of α-phase and ß-phase can be found, while the amount of carbides appear to be too small for giving a significant signal. Comparing the positions of the peaks, a shift can be observed between the pure Ti-22Nb alloy and the variant with an addition of 10wt% Zr.

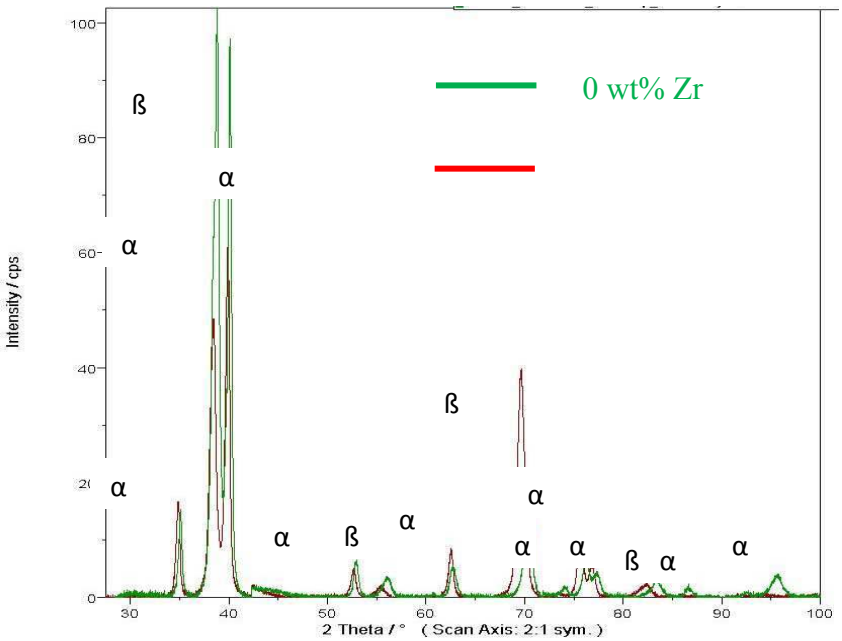

Fig.8 X-ray diffraction patterns of Ti-22Nb and Ti-22Nb-10Zr respectively

Table2 displays the calculated lattice parameters of α-phase and ß-phase of all the compositions prepared using MIM technique. It is visible that the lattice parameters in α- and ß-Ti phases are increased as zirconium is added to Ti-22Nb alloy. Thus, it can be concluded that the higher carbon solubility is due to a widening of the crystal lattice.

Table 2 Lattice parameters of Ti-22Nb-xZr (x=0, 2, 4, 6, 8, 10) calculated from XRD analysis

Latticeparameters a, c	ß-phase (BCC)	α-phase (HCP)	
Compositions	a (nm)	a (nm)	c (nm)
Ti-22Nb	0.32834±0.0002	0.29372±0.00217	0.47965±0.00354
Ti-22Nb-2Zr	0.32927±0.00136	0.29549±0.00048	0.48254±0.00078
Ti-22Nb-4Zr	0.33085±0.00097	0.29483±0.00260	0.48145±0.00425
Ti-22Nb-6Zr	0.33083±0.00106	0.29475±0.00215	0.48133±0.00351
Ti-22Nb-8Zr	0.33145±0.00049	0.29583±0.00234	0.48309±0.00382
Ti-22Nb-10Zr	0.33174±0.00063	0.29537±0.00233	0.48235±0.00380

Summary

Various characterization tests on specimens of Ti-22Nb, Ti-22Nb-xZr (x = 2, 4, 6, 8, 10) (wt%) prepared using Metal Injection Moulding were performed.

1. Uniform distribution of pores in all the alloys is observed, however, total porosity increased gradually from 3.1 % to 3.7 % with increasing Zr-content.

2. Ultimate tensile strength increased from 770 MPa to 850 MPa and yield strength from 670 MPa to 740 MPa for specimens with increasing zirconium content in Ti-22Nb alloy. Elongation to fracture of the specimens with higher zirconium content (6%-10%) was found to be in the range of 5 % elongation. Thus, a significant improvement compared to a previous work [19] was achieved.
3. Young' modulus has shown no significant variation and is around ~72 GPa for all compositions.
4. Metallographic evaluation has revealed the reduction of the carbide area fraction by Zr addition from 3.3% to 1.3%, while the grain size decreased from 299±143 μm to 225±111 μm.
5. The reason for the decrease in the amount of carbides was identified to be a probable increase in carbon solubility of the Ti matrix by widening of the crystal lattice. This could be proved by corresponding XRD measurements.
6. The combination of reasonable elongation, high tensile strength and lowYoung's modulus lets the alloy Ti-22Nb-10Zr processed by MIM appearing to be feasible for use as a biomedical implant material.

Reference

[1] Marc Long, H.J. Rack* Titanium alloys in total joint replacement—a materials science perspective Biomaterials 19 (1998) 1621-1639.

[2] M. Geetha, A. K. Singh, R. Ashokamani, A.K. Gogia, Ti based biomaterials, the ultimate choice for orthopaedic implants - A review. Progress in Materials Science 54 (2009) 397.

[3] David F. Williams, On the mechanisms of biocompatibility, Biomaterials, 30 (2009) 5897-5909.

[4] D. Mihov, B. Katerska, Some Biocompatible Materials Used in Medical Pratice, Trakia Journal of Science, 8 (2010) 119-125.

[5] L. Bolzoni,P.G. Esteban,E.M.Ruiz-Navas,E. Gordo, Mechanical behaviour of pressed and sintered titanium alloys obtained from master alloy addition powders, In Journal of the Mechanical Behaviour of Biomedical Materials15 (2012) 33-45.

[6] Euro PM 2011- Powder Injection Moulding: Process & Applications (MIM versus Investment Casting-Real Overlap for similar parts-Manuel Caballero, Technical Director ESRIMESA/MIMECRISA).

[7] Q.Wei, Influence of oxygen content on microstructure and mechanical properties of Ti–Nb–Ta–Zr alloy, Materials and Design, 32 (2011) 2934-2939.

[8] Y.H. Hon, J.Y. Wang, Y.N Pan, Composition/Phase Structure and Properties of Titanium-Niobium Alloys, Materials Transactions, 44 (2003) 2384-2390.

[9] M. Niinomi, Recent metallic materials for biomedical applications, Metallurgical and Materials Transcations A, 33 (2002) 477-486.

[10] K.K.Wang, Microstructure and properties of new beta titanium alloys, Ti-12Mo-6Zr-2Fe, developed for surgical implants, Medical Applications of Titanium and its Alloys, ASTM 1272, ASTM International (1996) 76-87.

[11] D. Mareci, R Chelariu, D.M. Gordin, G. Ungureanu, T. Gloriant,Comparative corrosion study of Ti-Ta alloys for dental applications, ActaBiomaterialia, 5 (2009) 3625-3639.

[12] Y.L. Zhou, M. Niinomi, T. Akahori, Dynamic Young's Modulus and Mechanical Properties of Ti–Hf Alloys, Materials Transactions, 45 (2004) 1549-1554.

[13] M. Tane, T. Nakano, S. Kuramoto, M. Hara, M. Niinomi, N.Akesue, T. Yano, H. Nakajima, Low Young's modulus in Ti–Nb–Ta–Zr–O alloys: Cold working and oxygen effects, Actamaterialia, 59 (2011) 6975-6988.

[14] D.Q. Martins, W.R. Osorio, M.E.P. Souza, R. Caram, A. Garcia, Effects of Zr content on microstructure and corrosion resistance of Ti–30Nb–Zr casting alloys for biomedical applications, ElectrochimicaActa, 53 (2008) 2809-2817.

[15] E.B. Taddei, V.A.R. Henriques, C.R:M. Silva, Carlos Cairo, Production of new titanium alloy for orthopedic implants, Materials Science and Engineering: C, 24 (2004) 683-687.

[16] D.R. Sumner, T.M. Turner, R. Igloria, R.M. Urban, J.O. Galante, Functional adaptation and ingrowth of bone vary as a function of hip implant stiffness, Journal of Biomechanics, 31 (1998) 909-917.

[17] Huihong Liu, MitsuoNiinomi, Masaaki Nakai, Junko Heida, Ken Cho, Bending springback behaviour related to deformation-induced phase tranformations in Ti-12Cr and Ti-29Nb-13Ta-4.6Zr alloys for spinal fixation applications, Journal of the Mechanical Behavior of Biomedical Materials, 34 (2014) 66-74.

[18] D. Zhao, K. Chang, T.Ebel, Ma Qian, R.Willumeit, Ming yan, F.Pyszak, Microstructure and mechanical behaviour of metal injection molded TI-Ni binary alloys as biomedical material,Journal of the Mechanical Behavior of Biomedical Materials, 28 (2013) 171-182.

[19] T.Beißig, Karbidausscheidungen bei ß-Titanlegierungen im MIM-Prozess, Masterarbeit (2014), in German.

[20] L. S. Moroz, B.B. Chechwlin, I.V. Dolin, L.V. Butalov, S.M. Shul'kin, A.P. Goryachev, TitaniumandItsAlloys, Sudpromgiz, Leningrad (1960) 185-190.

[21] G.A: Salishchev, S. Yu. Mironov, Effect of Grain Size on Mechanical Properties of Commercial Pure Titanium, Russian Physics Journal, 44 (6) (2001) 596-601.

[22] Y. Kawabe, S. Muneki, ‘Strengthening Capability of Beta Titanium Alloys, in : Beta Titanium Alloys of the 1990's’, D. Eylon et al. (eds.), TMS, Warrendale, PA, USA (1993) 187.

[23] Yuhua Li, CHao Yang, Haidong Zhao, Shengguan Qu, New Developments of Ti-Based Alloys for Biomedical Applications, Materials, 7 (2014) 1709-1800.

[24] Y. Okazaki, Y. Ito, A. Ito, T. Tateishi, ‘New Titanium Alloys To Be Considered For Medical Implant’, Medical Applications of Ti and Ti Alloys, S:A. Brown, J.E. Lemons, Eds., Medical applications of Ti and its alloys : The material and biological issues, STP 1272, AmericanSociety for Testing and Materials (1996).